Contrast Agent Distribution Function (CADF), a new dynamic MRI parameter from simultaneous measurement of relaxation rates R_1 and R_2* by a new Saturation-Recovery Multi-Gradient-Echo Snapshot sequence: Concept and first application to colorectal tumor xenografts in mice

M. Heilmann[1], J-L. Dimicoli[1], C. D. Thomas[1], C. Walczak[1], A. Volk[1]

[1]Integrative Imaging Unit, Institut Curie - Research Center, Orsay, France

Introduction: Dynamic MRI with T_1-weighted gradient echo sequences during administration of paramagnetic contrast agents (CA) is extensively evaluated to assess the potential of biomarkers characterizing tumor microvasculature. At high field strength and CA dose and/or relaxivity, R_2*-effects become more important. Simultaneous assessment of both, $R_1(t)$ and R_2*(t), by combining dynamic contrast-enhanced and susceptibility-contrast (DCESC) MRI, should increase information quality and content. In this study we introduce the contrast agent distribution function (CADF), a new parameter obtained by DCESC MRI, which provides specific information on susceptibility gradient evolution due to CA distribution. Using a new saturation-recovery multi-gradient-echo snapshot (SR-MGE-SNAP) sequence for simultaneous dynamic measurement of R_1 and R_2* [2], a preliminary in-vivo measurement of CADF in colorectal tumor xenografts in mice was performed.

Materiel and Methods: The CADF was defined as the contribution of temporal R_2*-changes, which arises from the heterogeneous distribution of a CA in tissue:

(1) $$\Delta R_2^*(t) = \Delta R_2(t) + \Delta R_2'(t) = r_2 \cdot C(t) + CADF(t)$$

In contrast to recent approaches dealing with $\Delta R_2'$ [1], the CADF explicitly considers CA extravasation into extravascular extracellular space (ees). Schematically, the CADF can be divided into two phases (Fig. 1): Phase I, characterized by rate constant k_a, describes the filling of microvessels with CA. Intravascular concentration (C_{iv}) results in a rising susceptibility gradient $\nabla\chi$ between vascular compartment (V_{iv}) and ees (V_{ees}) yielding an initial increase in CADF. Phase II reflects CA extravasation into ees at rate constant k_b. CADF was calculated from the relaxation rate ratio,

(2) $$\frac{\Delta R_2^*(t)}{\Delta R_1(t)} = \frac{r_2}{r_1} + \frac{CADF(t)}{\Delta R_1} \quad ,$$

by fitting a biexponential function with offset. Subsequently, CADF was modeled empirically by a pulse function:

(3) $$CADF(t) = (1 - A \cdot \exp(-k_a \cdot t)) \cdot B \cdot \exp(-k_b \cdot t) \quad .$$

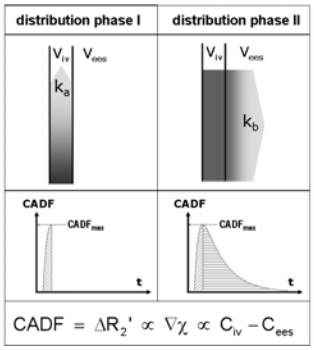

Fig.1: Contrast agent distribution function (CADF) – Schematic representation

Relaxation rates R_1 and R_2* were measured simultaneously by means of a SR-MGE-SNAP sequence (TR/TE/α/TS=12.6ms/2.2-9.6ms/14°/900ms,Δx=(0.5×0.5×2)mm^3), developed and validated with respect to classical IR-SE and MGE techniques on a 4.7T animal scanner (Bruker, Ettlingen) [2]. Signal intensities were extrapolated to TE=0ms by means of exponential fitting yielding R_2*. R_1 was calculated by applying the signal equation of a saturation-recovery sequence. Precontrast R_1 was determined in a variable saturation delay measurement before CA administration. In a preliminary study, eight nude mice with colorectal tumor xenografts (TC302, Institut Curie, France) were examined. For DCESC MRI a low molecular weight contrast agent (LMWM) (Dotarem®, Guerbet, France) was injected into the tail vein at a dose of 0.8mmol/kg (2µmol/s). CADF was determined in three different tumor regions: rim, intermediate and center.

Results: In Fig. 2 typical ΔR_1- and ΔR_2*-time courses observed in two tumors are shown: tumor A (a,b,c; V=68mm^3) and tumor B (d,e,f; V=204mm^3). In the rim of tumor A, ΔR_1 rose continuously (a) whereas ΔR_2* initially increased followed by a fast decrease (b). In the intermediate region both, R_1 and R_2*, reached a plateau which in case of R_1 stayed beneath changes of the rim, but were superior to latter for R_2*. In the center, both relaxation rates increased continuously but slower and with a lower maximum than in the outer regions. In tumor B, ΔR_1 rose continuously in all regions (d), however, with smaller initial slope and maximum for regions closer to center. In contrast, ΔR_2* showed similar behaviour in all regions (e), with a slightly lower maximum in the rim compared to the inner regions.

CADF could be determined in all regions of all tumors, and for the LMWM biphasic behaviour was always observed. Good fitting results were obtained when applying the proposed pulse function (Eq. 3) with following mean/minimum/maximum R^2-values: rim=0.995/0.991/0.999, intermediate=0.989/0.972/0.998 and center=0.829/0.406/0.963. In tumor A, $CADF_{max}$ of the rim was higher than those of the intermediate and center region (c), whereas in tumor B, $CADF_{max}$ was highest in the tumor center (f). In all animals k_b decreased continuously from tumor periphery towards the center.

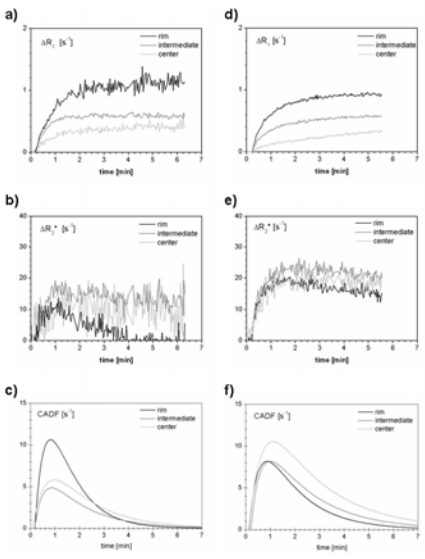

Fig. 2: ΔR_1- (a,d) and ΔR_2-(b,e) time courses and CADF (c,f) observed in three different regions of two tumors of different volumes (left and right column)*

Discussion/Conclusion: The SR-MGE-SNAP sequence is a robust technique for simultaneous dynamic measurement of $R_1(t)$ and R_2*(t) opening the field of DCESC MRI by combining DCE with DSC MRI, and therefore enhancing information quality and content. In a preliminary study, different ΔR_1- and ΔR_2*-time courses were observed in each tumor indicating the complementary information content of both relaxation rates. Excellent fitting of measured CADF to the empirical model function confirmed the biphasic distribution kinetics. Corresponding parameters (k_a,$CADF_{max}$,k_b), determined without the need of *in situ* relaxivities and estimation of CA concentration, should be related to tumor blood flow (k_a), tumor blood volume and microvascular architecture ($CADF_{max}$), and CA diffusion into the ees (k_b). These new parameters are expected to have high potential for monitoring changes of vascular properties during antivascular/antiangiogenic treatment.

References: [1] Kiselev VG, Strecker R, Ziyeh S, Speck O, Hennig J. Magn Reson Med 2005; 53:553-563. [2] Heilmann M, Dimicoli JL, Thomas CD, Walczak C, Volk A. Proc. ESMRMB 2006; 413

Acknowledgements: This work was supported by the French "*Institut National du Cancer*", the "*Cancéropôle Ile de France*", the Promoting Research Program "*Anti-tumor vectorization*" and the grant no. ACI033159 of the French Research Ministry.